Spatiotemporal path-matching for comparisons between ground-based and satellite lidar measurements

Correlación espacio-temporal para comparación entre medidas de lidares de superficie y satelitales

Timothy A. Berkoff[1], Sandra Valencia[2], Ellsworth J. Welton[3], and James D. Spinhirne[3]

1.Goddard Earth Science and Tech. Center, UMBC, Code 613.1, Greenbelt, MD USA
2. SSAI Inc., NASA GSFC Code 613.1, Greenbelt, MD USA
3. NASA Goddard Space Flight Center, Greenbelt, MD USA

ABSTRACT:

The spatiotemporal sampling differences between ground-based and satellite lidar data can contribute to significant errors for direct measurement comparisons. Improvement in sample correspondence is examined by the use of radiosonde wind velocity to vary the time average in ground-based lidar data to spatially match coincident satellite lidar measurements. Results are shown for the 26 February 2004 GLAS/ICESat overflight of a ground-based lidar stationed at NASA GSFC. Statistical analysis indicates that improvement in signal correlation is expected under certain conditions, even when a ground-based observation is mismatched in directional orientation to the satellite track.

Las diferencias espacio-temporales en el muestreo de datos de lidars de superficie terrestres y satelitales pueden contribuir a errores significativos en las comparaciones directas de las mediciones. El mejoramiento en la correlación del muestreo es examinado con el uso de la velocidad del viento, obtenida por medio de radiosondas, con el objetivo de variar el promedio en tiempo de las mediciones de lidares de superficie para correlacionar espacialmente las mediciones coincidentes de lidares satelitales. En este artículo se mostrarán los resultados del sobrevuelo del lidar GLAS en el satélite ICESat sobre un lidar de superficie ubicado en NASA GSFC el 26 de Febrero de 2004. Un análisis estadístico indica que se espera un mejoramiento en la correlación de la señal bajo ciertas circunstancias, incluso cuando las trayectorias del viento y el satélite no coinciden en orientación.

Keywords: Lidar, Aerosols, Clouds, Satellite, Measurements

REFERENCES AND LINKS.

[1] J.C. Antuna et. al., "Toward a lidar network in Latin America", Proc. Twenty-First International Laser Radar Conference (ILRC21): (vol.) 345-7, 2002
[2] see http://lidarb.dkrz.de/earlinet/
[3] see http://mplnet.gsfc.nasa.gov/

1. Introduction

One of the key motivations for the establishment of ground-based lidar networks such as the Americas Lidar Network (ALINE) [1], European Aerosol Research Lidar Network (EARLINET) [2], and the Micro-Pulse Lidar Network (MPLNET) [3] is to contribute towards the calibration and validation of satellite-based measurements. However, direct comparisons between surface and space-borne measurements is complicated due to the spatial and temporal differences between measurements. Both the Geoscience Laser Altimeter System (GLAS/ICESat) and the Cloud-Aerosol Lidar and Infrared Pathfinder Satellite Observation (CALIPSO) lidars pass over ground sites at ~ 7 km per second, while ground-based lidars typically obtain measurements with a stationary vertical-pointing beam. Consequently, direct temporal overlap between lidar measurements is extremely brief, and signal averaging of satellite data outside

the coincident sample volume will introduce unknown errors due to atmospheric dynamics. This is particularly true for cloud backscatter properties which are often highly variable over short temporal and spatial scales. In this paper, a method using wind velocity information to improve the spatiotemporal correspondence between coincident surface lidar and satellite measurements is examined. Spatial-constant lidar profiles are generated from ground-based measurements by adjusting the temporal average in each range-bin to maintain a constant advection path length, as determined by wind velocities from radiosonde data. Under conditions where advection is the dominant source of atmospheric motion, this approach is expected to improve sample representation, and allow for extended signal averaging intervals.

2. MPL and GLAS Lidars

For this study, data from GLAS/ICESat satellite and ground-based Micro-Pulse Lidar (MPL) are examined. Table 1 summarizes the key characteristics between the two different systems. MPLs are elastic-backscatter lidars suitable for deployment at remote sensing locations due to the eye-safe transmitted energy and small size. Eye-safe transmission is achieved by expanding a rapidly pulsed 523 nm laser source through a 20 cm diameter Cassegrain-type telescope. Atmospheric backscatter is collected through the same telescope, with the signal return being detected by an avalanche photodiode. Signal-to-noise performance is optimized through the use of a high repetition rate (2500 Hz) laser, narrow field-of-view (100 urad), and narrow bandpass filters (0.2 nm). The laser beam divergence is approximately 15 urad (full angle), resulting in a beam diameters less than 1 meter for measurements in the troposphere.

TABLE I

	ICEsat/GLAS (Atmospheric Channel)	Micro-Pulse Lidar (standard MPLNET config)
Wavelength	532 nm	523 nm
Laser Repetition Rate	40 Hz	2500 Hz
Beam Diameter (at surface)	70 meters	0.2 meters
Beam Divergence	100 urad	15 urad
Field of View	200 urad	100 urad
Beam spatial velocity	~ 7 km/sec	Stationary (non-scanning)

The GLAS/ICESat satellite was launched in January 2003 and placed into polar orbit ~ 600 km in altitude. Its primary purpose is to provide high precision altimetry measurements on a global basis using a 1064 nm laser source. A second wavelength, at 532 nm, is also transmitted and is used for atmospheric backscatter measurements of clouds and aerosols. This wavelength is sufficiently close to the MPL wavelength to enable direct comparisons of backscatter. The GLAS laser beam has a surface footprint diameter of approximately 70 meters and can be pointed up to +/- 5 deg from the nadir satellite ground track with an accuracy of +/- 50 meters. The beam output has a pulse repetition rate of 40 Hz, and passes over surface positions at a velocity of ~ 7 km/sec resulting in ~ 170 meter separation between the laser pulses. The receiver has a 200 urad field of view that is ~2x larger than the MPL receiver.

3. GLAS-MPL Coincident Data Set

On 26 February 26, 2004 at 08:54 UT, GLAS/ICEsat passed over the NASA Goddard Space Flight Center (GSFC) located in Greenbelt, Maryland (USA). This location is a MPLNET site, and simultaneous ground-based MPL measurements were recorded during this overpass. Although the satellite nadir track was to the west of GSFC, GLAS/ICESat was pointed to the GSFC location for this overpass, resulting in the measurement ground track directly passing over the site with a high degree of spatial accuracy.

Figure 1 shows the resultant backscatter observations from both from GLAS/ICESat and the MPL. The MPL data are shown for +/- 1 hour duration about the 08:54 UT satellite overpass and has 1 minute time and 75 meter vertical resolution. The GLAS/ICESat 532 nm backscatter data are presented for +/-50 km travel distance about the MPL location and has 0.2 second temporal resolution (1.36 km spatial distance), and 75 meter vertical resolution. Signal magnitude for both measurements are independently calibrated in units of attenuated backscatter. As seen from the lidar images, cirrus were present from 7 to 10 km, and exhibited a high degree of structural variability. Signal attenuation through the cirrus layer was relatively low, reducing the need to account for profile attenuation shape differences due to the upward and downward viewing measurements.

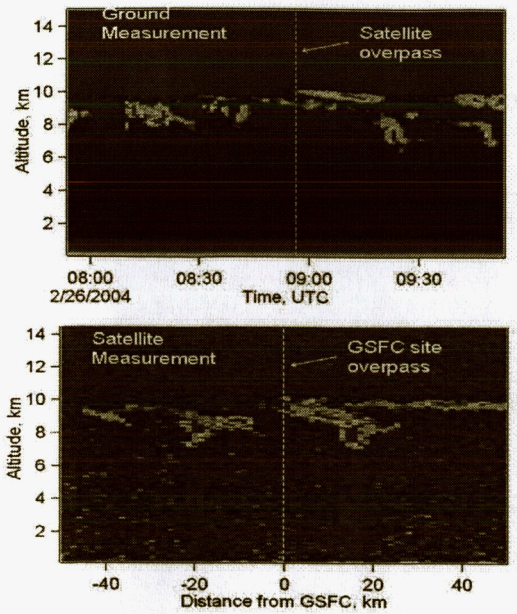

Fig. 1. Attenuated backscatter images from the MPL (top) and GLAS (bottom) for the 26 Feb. 2004 overpass.

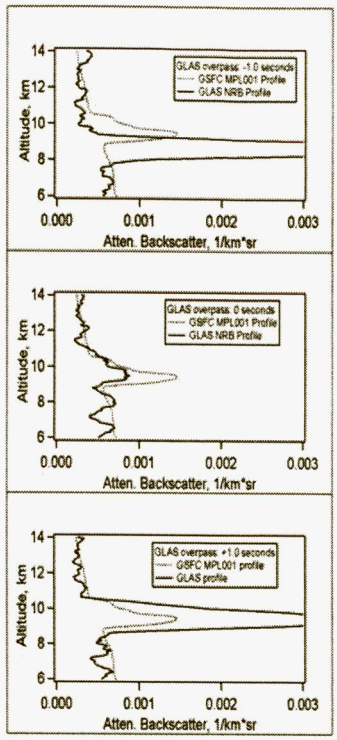

Fig. 2. . Profile plots for the MPL 08:54 UT 1 minute profile (dashed) and 1 second average GLAS profiles (solid) for a sequence of three 1-second intervals before (top), during (center), and after (bottom) GSFC overpass. Profiles shown are box-car averaged to 0.7 km vertical resolution.

Figure 2 shows 1 second time averaged (6.8 km ground track) backscatter profiles for three different cases: 1 second before (from -10 to -3.4 km), during (- 3.4 to 3.4 km), and 1 second after (+3.4 to 10 km) coincidence with the MPL location. Also shown is the 1-minute MPL profile taken during overpass time (08:54 UT). Profiles shown are box-car averaged to 0.7 km vertical resolution in order to reduce the noise present on the GLAS data. For the coincident case, a drop in GLAS measured cirrus intensity occurs more closely matching the 08:54 MPL profile when compared to the +/-1 second (+/- 6.8 km) before and after cases. Relatively good signal agreement can be seen in the stable Rayleigh (molecular) signal levels above and below the cirrus layer, signifying cross-validation of the independently determined calibrations for these lidars.

4. Radiosonde Data

To better determine the spatiotemporal relationship between the MPL and GLAS observations, radiosonde information was obtained from the NOAA RAOB Forecast Systems Laboratory database. In the altitude range of the cirrus, the dominant source of atmospheric motion is due to the mid-latitude jet-stream. Figure 3 shows direction and horizontal wind velocity from the IAD radiosonde launch site (WMO station #72403) for 26 February 12:00 UT, approximately 55 km to the west of NASA GSFC. Examination of additional radiosonde profile launched at 11:00 UT from the APG site (WMO station #74002), 90 km to the northeast showed nearly identical data in the 7 to 12 km altitude range, indicating consistent west-to-east wind direction with ~1 km/min horizontal velocity at the base and ~3 km/min at the top of the cirrus layer. These velocities provide significant cloud motion over the MPL site, allowing for the observational time domain to be related to a spatial path length.

5. Spatial-constant lidar profiles

In this study, "spatial constant" lidar profiles are generated from the ground-based MPL measurements by varying the temporal average at each altitude bin to maintain a constant advection path length (CAPL). Figure 4 shows four different CAPL profiles (20, 50, 100, and 200 km) based on the IAD radiosonde wind velocity profile from Figure 3. The time average range in the CAPL profiles are centered about the 08:54 UT

coincidence with GLAS. For each CAPL case, a GLAS profile with its corresponding spatial distance average centered about coincidence is also shown. Although these observations are matched in length for the GLAS-MPL profile plots, the measurement path directions are not. The GLAS track is oriented close to the north-south direction while the MPL observation is oriented towards the westerly direction of the jet-stream, further reducing signal correlation. However, statistical agreement between signals would be possible if the cloud structure over the region was consistent and the measurement distance was long enough to reflect a representative sample for the region. For the spatial constant MPL-GLAS profile comparisons, a significant improvement in profile agreement is seen in the 200 km spatial average when compared to shorter path-length cases. It is unclear from these plots alone if this improvement is due to a true convergence to a representative profile for the region, or the result of statistical anomaly. Figure 5 shows the MPL and GLAS profile averages over a continuum of distance intervals about coincidence, illustrating the signal convergence behavior for both data sets. For this result, MPL CAPL and GLAS signal averages are represented by color intensity in units of attenuated backscatter. For very short distance intervals (< 12 km) where correlation is expected, profile agreement between the GLAS and MPL data sets can be seen. For distance intervals beyond 12 km, the differences between the two images increases, as uncorrelated cloud contributions begin to dominate. As the distance-interval is increased beyond 100 km, both data sets begin to converge to a more stable solutions, resulting in the quasi-matched profiles observed at 200 km.

6. Monte-Carlo Simulation

To further examine two spatially intersecting but directionally different measurement paths, a Monte-Carlo analysis was used to investigate signal response in a simulated cloud field. This analysis is based on a simple digital (signal/no signal) representation of clouds randomly distributed in a horizontal atmospheric plane. Although not intended to simulate actual backscatter properties from cirrus clouds, this elementary approach can illustrate the signal statistical dependence on distance-interval for different directional paths. Figure 6(a) shows an example 200 x 200 km grid with randomly distributed 8 km features at a density that results in an equivalent cloud fraction of 0.27. As illustrated, two different intersecting measurement paths through the cloud field can be used to imitate the MPL (P1) and GLAS (P2) observations. Figure 6(b) shows the resultant standard deviation in

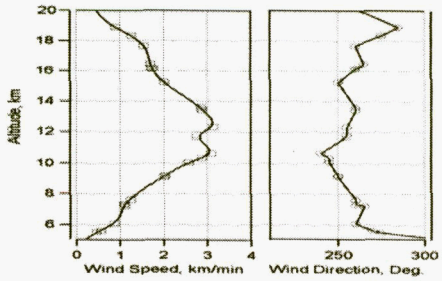

Fig. 3. Radiosonde data for the 26 February 12:00 UT launch from IAD (WMO station #72403).

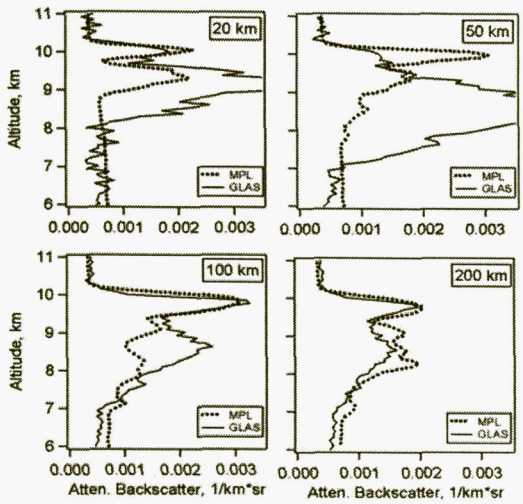

Fig. 4. Backscatter profiles for GLAS (solid) and MPL (dashed) for four different distance intervals (20, 50, 100, and 200 km) about coincidence.

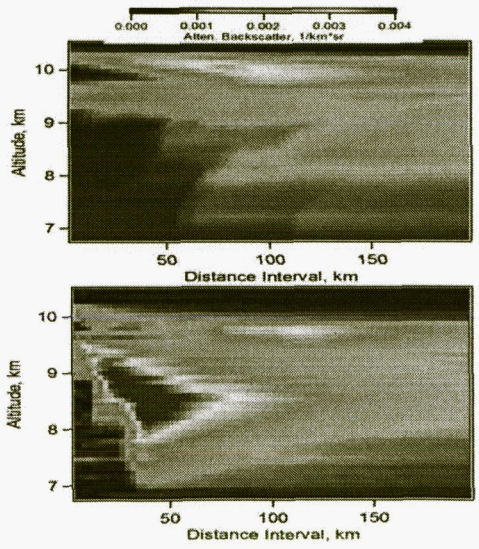

Fig. 5. MPL (top) and GLAS (bottom) profiles for different distance averaging intervals centered on the 08:54 UT MPL-GLAS coincidence on 26 Feb 2004.

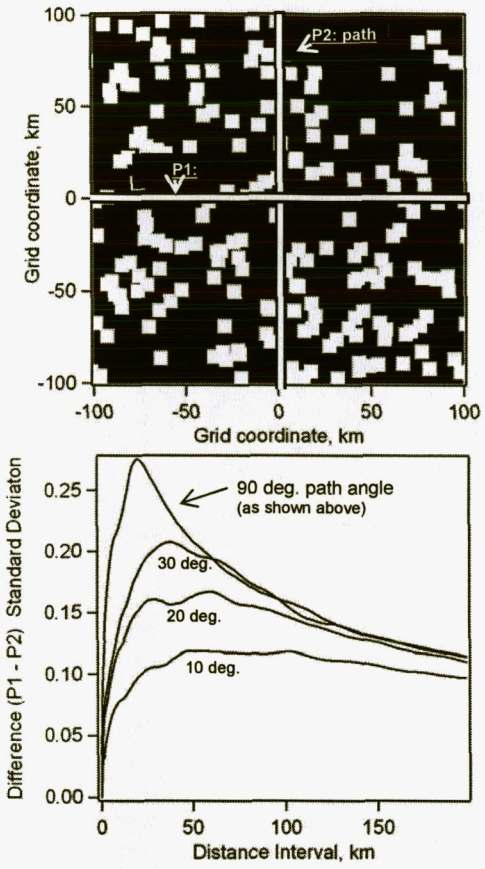

Fig. 6(a) & (b). Top image (a) cloud scene example used in Monte-Carlo analysis. MPL and GLAS measurement tracks represented by path P1 and P2 respectively. Bottom plot (b) is the deviation in signal difference (P1-P2) from a trial of 2500 cloud scenes.

signal differences (P1 – P2) from a trial of 2500 cloud fields where distance averaging intervals between 0 to 200 km were evaluated for each scene. The result describes the kind of signal behavior present in the lidar distance-interval images in Figure 5. For extremely short distance-intervals (less than 20 km), the deviation between signals is low, as expected for short signal path averages close to the intersection at the center of the field. As distance-interval is increased about coincidence, the deviation between the two measurements increases, as uncorrelated features contribute to the signal average. After reaching a maximum, the signal differences decrease as the sampling of both paths begin to converge on the statistical mean for the full field. The most pronounced variance is seen for the orthogonal case (90 deg.). This is the directional case that most closely imitates the 26 February GLAS-MPL overpass. Despite the degree of mismatched direction in paths, the Monte-Carlo results do illustrate the possibility of improved lidar correlations by extending the signal average interval. Reducing the path angle between P1 and P2, the deviation (shown for 30, 20, and 10 deg. cases in Fig. 6(b)) diminishes as the two measurement paths begin to geometrically align. Other cloud sizes and densities were also evaluated producing similar looking set of functions. However, to accurately quantify the true statistical behavior, a more sophisticated cloud scene description is needed that factors in cloud size distribution and other signal properties. An improved model incorporating these features is currently being pursued.

7. Conclusions

The spatiotemporal relationship between satellite and ground-based lidar measurements is an important factor in determining signal correlation. Incorporation of wind information can improve signal correspondence under certain conditions, by transforming ground-based lidar data from the temporal to the spatial domain. Using this approach, constant path-length profiles were generated from a ground-based MPL and compared to coincident GLAS data for an overpass case on 26 February 2004. Results show GLAS-MPL profile correlation for a 200 km spatial path, despite the directional differences in observations. A simple statistical model was used to illustrate signal correlation for different distance intervals and direction orientations in a random field. Further enhancements in statistical modeling and additional measurement comparisons will help to define signal correlation for different atmospheric conditions and averaging intervals. Spaceborne lidars such as GLAS and CALIPSO provide unique opportunities to investigate spatiotemporal applications for ground-based lidar networks, the results of which could be extended to other earth observing satellites such as MODIS, MISR and TOMS.

8. Acknowledgements

The authors gratefully acknowledge radiosonde data provided by the by the NOAA RAOB Forecast Systems Laboratory, Steve Palm for providing GLAS data, and Dennis Hlavka for helpful discussions. This work is supported by the NASA Earth Observing System (EOS) and the NASA Radiation Sciences Program.